THE JOURNAL OF BIOLOGICAL CHEMISTRY
Vol. 278, No. 10, Issue of March 7, pp. 7863–7874, 2003

Printed in U.S.A.

Kinetic and Catalytic Properties of Dimeric *Kpn*I DNA Methyltransferase*

Received for publication, November 11, 2002, and in revised form, December 19, 2002
Published, JBC Papers in Press, December 28, 2002, DOI 10.1074/jbc.M211458200

Shivakumara Bheemanaik‡, Siddamadappa Chandrashekaran§, Valakunja Nagaraja§, and Desirazu N. Rao‡¶

From the ‡Department of Biochemistry, and §Department of Microbiology and Cell Biology, Indian Institute of Science, Bangalore 560012, India

***Kpn*I DNA-(N^6-adenine)-methyltransferase (*Kpn*I MTase) is a member of a restriction-modification (R-M) system in *Klebsiella pneumoniae* and recognizes the sequence 5′-GGTACC-3′. It modifies the recognition sequence by transferring the methyl group from *S*-adenosyl-L-methionine (AdoMet) to the N^6 position of adenine residue. *Kpn*I MTase occurs as a dimer in solution as shown by gel filtration and chemical cross-linking analysis. The nonlinear dependence of methylation activity on enzyme concentration indicates that the functionally active form of the enzyme is also a dimer. Product inhibition studies with *Kpn*I MTase showed that *S*-adenosyl-L-homocysteine is a competitive inhibitor with respect to AdoMet and noncompetitive inhibitor with respect to DNA. The methylated DNA showed noncompetitive inhibition with respect to both DNA and AdoMet. A reduction in the rate of methylation was observed at high concentrations of duplex DNA. The kinetic analysis where AdoMet binds first followed by DNA, supports an ordered bi bi mechanism. After methyl transfer, methylated DNA dissociates followed by *S*-adenosyl-L-homocysteine. Isotope-partitioning analysis showed that *Kpn*I MTase-AdoMet complex is catalytically active.**

Prokaryotic DNA methyltransferases (MTases)[1] are usually components of restriction-modification (R-M) systems that enable cells to resist propagation of foreign genomes that would otherwise kill them (1). DNA methylation is catalyzed by *S*-adenosyl-L-methionine (AdoMet)-dependent DNA methyltransferases. Based on the position of methyl group transfer on bases in DNA, DNA MTases are classified into two groups, exocyclic or amino methyltransferases and endocyclic or ring methyltransferases (2). The amino methyltransferases methylate exocyclic amino nitrogen and form either N^6 methyladenine or N^4 methylcytosine, whereas ring methyltransferases methylate ring carbon and form C^5 methylcytosine. All exocyclic MTases share a common architectural plan. They have nine highly conserved motifs, and these can be arranged in different combinations (3). The amino methyltransferases are further subdivided into three groups, namely α, β, and γ, which are characterized by a distinct linear order of the AdoMet binding region (F*X*G*X*G), target recognition domain, and catalytic (DPPY) motif. Target recognition domains are long sequences containing no conserved amino acids. The low amino acid sequence similarity between target recognition domains explains the specificity of a particular methyltransferase for a specific sequence.

Several type I and type II R-M systems have been isolated from strains of *Klebsiella pneumoniae*. These include *Kpn*I, *Kpn*K14I (an isoschizomer of *Kpn*I), *Kpn*2I (an isoschizomer of *Bsp*MII), *Kpn*49kI (an isoschizomer of *Eco*RI), *Kpn*49kII (an isoschizomer of *Nci*I), and various yet unnamed enzymes that are isoschizomers of *Eco*RII, *Bss*HII, and *Pst*I (4). Although the type I systems includes *Kpn*AI (5) and *Kpn*BI (6), *Kpn*I restriction-modification system belongs to the type II R-M systems. The genes for *Kpn*I endonuclease and methyltransferase are present within close proximity to each other in *K. pneumoniae* genome (7). *Kpn*I MTase recognizes the recognition sequence 5′-GGTACC-3′ (8) and modifies the DNA by methylating the adenine residue at the N^6 position (9). Based on the conserved motif arrangement, *Kpn*I MTase belongs to the β-subgroup of MTases. Comparison of the amino acid sequence of *Kpn*I MTase with the sequences of various MTases revealed a significant homology with N^6-adenine MTases and partial homology with N^4-cytosine MTases but no sequence homology with C^5-cytosine MTases. Dot matrix comparison of *Kpn*I MTase with several N^6-adenine MTases and N^4-cytosine MTases showed that it has homology with the catalytic motif (DPPY) and AdoMet binding motif (F*X*G*X*G) of most N^6-adenine MTases and only the F*X*G*X*G region of N^4-cytosine MTases. Interestingly, the amino acid sequence of *Kpn*I MTase is more closely related to those of *Eco*P1 MTase and *Eco*P15I MTase, which belong to type III R-M systems (7). Among all the MTases characterized so far, most of them are monomers, whereas their cognate endonucleases are dimers.

Kinetic mechanisms of C^5 MTases such as *Hha*I (10–13), murine DNMT1 (14), *Msp*I (15), human DNMT1 (16), and mammalian DNMT3a (17) have been determined. All known cytosine methyltransferases studied so far follow an ordered bi bi mechanism with DNA as the leading substrate. Kinetic mechanisms for members of the N^4 cytosine MTase family such as *Pvu*II and N^6-adenine MTases such as *Eco*P15I (18), *Eco*RI (19, 20), *Rsr*I (21), *Eca*I (22), *Ccr*M (23), *Taq*I (24), *Eco*RV (25), and T4 Dam (26) have also been elucidated. Bacterial N^6-adenine methyltransferases, in general, exhibit different kinetic mechanisms.

Our aim is to study the interaction between DNA and *Kpn*I MTase by kinetic analysis of the enzymatic reaction. In the present study we report the oligomeric nature of *Kpn*I MTase

* This work was supported by a grant from Department of Science and Technology, Government of India. The costs of publication of this article were defrayed in part by the payment of page charges. This article must therefore be hereby marked "*advertisement*" in accordance with 18 U.S.C. Section 1734 solely to indicate this fact.

¶ To whom correspondence should be addressed. Tel.: 91-80-3942538; Fax: 91-80-3600814; E-mail: dnrao@biochem.iisc.ernet.in.

[1] The abbreviations used are: MTase, DNA methyltransferase; AdoMet, *S*-adenosylmethionine; AdoHcy, *S*-adenosylhomocysteine; DE81, diethylaminoethyl ion-exchange filters; R-M, restriction-modification; DNMT, DNA MTase.

Oligonucleotide Sequence	Duplex
5′-ATTGCGT**GATACC**CGCTCTT-3′	I
5′-ATTGCGT**GGAACC**CGCTCTT-3′	II
5′-ATTGCGT**GTTACC**CGCTCTT-3′	III
5′-ATTGCGT**GGTCCC**CGCTCTT-3′	IV
5′-ATTGCGT**GGTACG**CGCTCTT-3′	V
5′-ATTGCGT**TGTACC**CGCTCTT-3′	VI
5′-ATTGCGT**GGATCC**CGCTCTT-3′	VII
5′-ATTGCGT**GGTACC**CGCTCTT-3′	VIII
5′ -GAGAGGCGGTTTGCGT**GGTACC**CGCTCTTCCGCTTCCT-3′	IX
5′-GAGAGGCGGTTTGCGT**GGTAC**^{CH_3}**C**CGCTCTTCCGCTTCCT-3′	X
5′ -B**TGGGAAGCGGGTACC**TGAATTCTT-3′ 3′ -ACCCTTCGC**CCATGG**ACTTAAGAA-5′	XI

FIG. 1. **Duplex substrates.** Duplexes I–VII are noncanonical oligonucleotides for *Kpn*I MTase recognition sequence. Duplex VIII (20-mer) and IX (38-mer) are oligonucleotides containing canonical sequences, whereas duplex X is a hemimethylated oligonucleotide sequence of *Kpn*I MTase. A complementary strand was used for all the oligonucleotides. In duplex XI, *B* represents biotin labeled at the 5′ end.

using gel filtration, chemical cross-linking, and enzyme concentration-dependent analysis. The kinetic parameters for methylation reaction with DNA substrates of different length by *Kpn*I MTase have been determined. We also report the order of substrate binding and product release using initial velocity dependence analysis, product inhibition, substrate inhibition, and steady state kinetic analysis. Our results demonstrate that *Kpn*I MTase exists as a dimer in solution and functions as a dimer during the methylation reaction. The methylation reaction proceeds through a steady state ordered bi bi kinetic mechanism in which AdoMet binds first followed by DNA.

EXPERIMENTAL PROCEDURES

Bacterial Strains and Plasmids Used—Escherichia coli stain DH10B [*mcrA*Δ(*mrr hsd* RMS *mcr*BC) *end*A1 080 *dlac*Z ΔM15 Δ*lac* X74 *rec*A1 *deo*RΔ (*ara, leu*) 7697*ara* D139 *gal*U *gal*K *nup*G *rps*L] was used as a host strain for transformation of pACMK clones, which encode *Kpn*I MTase (27).

Enzymes and Chemicals—Restriction and modifying enzymes were purchased from New England Biolabs. *S*-Adenosyl-L-[^{3}H]methionine (78.9 Ci/mmol) was purchased from PerkinElmer Life Sciences, and AdoMet, chloramphenicol, bovine serum albumin, HEPES, polyethyleneimine, Coomassie Brilliant Blue, RNase A, glutaraldehyde, and *S*-adenosyl-L-homocysteine (AdoHcy) were purchased from Sigma. AdoHcy was prepared by dissolving 38.44 mg into 1 ml of 1 N HCl to give a 100 mM solution. Dilutions were made fresh in distilled water. Phosphocellulose P11 and DE81 anion-exchange filter papers were purchased from Whatman. All other chemicals used were of highest grade purity. Centricon 10 microconcentrator units were purchased from Amicon. Oligonucleotides for methylation assays were purchased from Microsynth GmbH, Switzerland and Bangalore Genei Pvt. Ltd., India. Oligonucleotides used in this study are listed in Fig. 1. Double-stranded DNA concentration was measured spectrophotometrically, assuming an A_{260} of 1.0 to correspond to 50 μg/ml for double-stranded DNA.

*Expression and Purification of KpnI MTase—Kpn*I methyltransferase was expressed in *E. coli* DH10B cells containing plasmid pACMK (27). *E. coli* cells harboring *Kpn*I MTase clone pACMK were grown for 12–16 h at 37 °C in LB medium containing 20 μg/ml chloramphenicol, and cells were harvested by centrifugation for 10 min at 10,000 rpm. Harvested cells (10 g) were suspended in 20 ml of buffer A (10 mM potassium phosphate, pH 7.0, 1 mM EDTA, 100 mM KCl, and 7 mM β mercaptoethanol) and sonicated. Care was taken that the temperature during sonication was maintained at 4 °C. Unless indicated otherwise, all steps were carried out at 0–4 °C. The sonicated cell suspension was centrifuged at 100,000 × *g* for 2 h. The crude extract was treated with 1% (v/v) polyethyleneimine in the presence of 250 mM KCl. The sample was centrifuged at 10,000 rpm, and the supernatant was subjected to 0–30% ammonium sulfate fractionation. The pellet was dissolved in buffer A, dialyzed, and loaded onto a phosphocellulose column previously equilibrated with buffer A. The enzyme was eluted with a linear gradient of 0.1-1 M KCl. Fractions containing the enzyme were pooled and dialyzed against buffer B (10 mM Tris-HCl, pH 7.4, 0.1 mM EDTA, 100 mM KCl, 7 mM β-mercaptoethanol, and 10% glycerol). Dialyzed sample was loaded onto a heparin-Sepharose column equilibrated with buffer B and eluted with a linear gradient of 0.1–1 M KCl. Fractions containing enzyme were pooled and dialyzed against buffer B containing 50% glycerol, and the enzyme was stored at −20 °C. The purity of the protein was judged as being greater than 99% on SDS-PAGE, and the yield of purified *Kpn*I MTase from 10 g of cells was ~5 mg. Purified *Kpn*I MTase was stable for at least 3 months at −20 °C. Protein concentration was estimated by the method of Bradford (28) using bovine serum albumin as standard.

Methylation Assay—All methylation assays monitored incorporation of tritiated methyl groups into DNA by using a modified ion-exchange filter assay (29). Reactions contained 100 mM HEPES, pH 8.0, 0.25 mM EDTA, and 11 mM β-mercaptoethanol. Enzyme and substrate concentrations (DNA and AdoMet) were used as noted in each experiment. After the incubation of enzyme and substrates at 37 °C, reactions were stopped by transferring aliquots onto small Whatman DE81 filter paper discs. Filters were washed 3 times (5 min each) with 0.2 M ammonium bicarbonate solution equilibrated at 4 °C, once with 95% (v/v) ethanol, and once with diethyl ether. Filters were air-dried, and the tritium content was determined in 3 ml of scintillation fluid (0.5% 2,5-diphenyloxazole and 0.05% 1,4-bis[2-(5-phenyl-oxazoyl)] benzene in 1:1 (v/v) 2-methoxyethanol and toluene) using an LKB Rack BETA model II liquid scintillation counter. All data are corrected for nonspecific binding of [^{3}H]AdoMet to the washed filter. Background counts were measured at zero-time incubation, the incubation in the absence of enzyme was subtracted (less than 100 cpm), and data were analyzed. The amount of enzyme that transferred 1 nmol of [^{3}H]methyl group to the substrate DNA was, thus, obtained. One unit of *Kpn*I MTase activity was defined as the amount of enzyme that incorporated 1 nmol of [^{3}H]methyl group into the DNA/min at saturating concentrations of substrates at 37 °C. The specific activity of *Kpn*I MTase is referred to as units/mol of protein; that is, nmol of [^{3}H]methyl groups/min/mol of protein.

Gel Filtration Analysis of KpnI MTase—Native molecular mass of *Kpn*I MTase was determined by gel filtration analysis and performed on a Superdex 200 column in buffer B. To determine the molecular mass of *Kpn*I MTase, the column was calibrated with suitable molecular weight markers ranging from 12 to 150 kDa. The void volume (V_o) of the column was found to be 40 ml, and the bed volume was 120 ml. The elution volumes (V_e) of marker proteins and *Kpn*I MTase were determined. The molecular mass of *Kpn*I MTase was calculated from the plot of V_e/V_o *versus* log molecular weight.

*Chemical Cross-linking of KpnI MTase—Kpn*I MTase (4.44 μM) was incubated on ice for 15 min. Increasing amounts of glutaraldehyde were then added to the protein solution to a final concentration range of 0.05–0.5%, and the mixture was further incubated on ice for 1 h. Reaction products were separated by electrophoresis on a denaturing polyacrylamide gel (0.1% (w/v) SDS, 10% (w/v) polyacrylamide) and visualized by silver-staining.

Preincubation Studies—Preincubation experiments were carried out by incubating 1 μM *Kpn*I MTase with either 1 μM DNA or 2 μM [^{3}H-methyl]AdoMet at 37 °C for 5 min. The reaction was initiated by adding AdoMet or DNA, respectively. At 10-, 20-, 30-, 40-, 50-, and 60-s time intervals, 20-μl aliquots were removed and analyzed for product formation using the DE81 filter binding assay. In a control experiment, AdoMet and DNA were preincubated at 37 °C for 5 min, and the reaction was started with *Kpn*I MTase.

Determination of Kinetic Parameters—Kinetic studies were done using pUC18 supercoiled plasmid DNA. Methylation assays were carried out as described earlier for 2.5 min to determine initial velocity dependence. In a series of similar reactions containing *Kpn*I MTase (1 μM) and [^{3}H]AdoMet (2 μM), the concentration of DNA was varied in the range of 50 nM–1 μM. A double reciprocal plot of the initial velocity *versus* DNA concentration allowed the determination of K_m^{DNA} and V_{max}. Similarly, initial velocity experiments were carried out by varying the concentration of [^{3}H]AdoMet in the range of 50 nM–2 μM while keeping the DNA concentration fixed at 1 μM and keeping other reaction conditions identical. The double reciprocal plot of initial velocity *versus* [^{3}H]AdoMet concentration allowed the determination of K_m^{AdoMet} and V_{max}. The turnover number (k_{cat}) was calculated as the ratio of V_{max} to

the enzyme concentration used. The kinetic constants were also calculated for the *Sca*I-linearized pUC18 DNA, unmethylated oligonucleotide (38-mer), and hemimethylated oligonucleotide (38-mer). Data obtained were plotted by regression analysis using Sigma Plot. The equations used to obtain the kinetic constants, V_{max}, K_m^{DNA} K_m^{AdoMet}, and k_{cat} were as described (30, 31). Unless otherwise indicated, all enzyme activity data were the average of at least triplicate determinations.

Initial Velocity Dependence on DNA and AdoMet—Methylation assays were carried out to determine the initial velocity dependence of DNA and AdoMet as described earlier. In a series of identical reactions containing 1 μM *Kpn*I MTase and 250 nM AdoMet, the concentration of the substrate DNA was varied in the range of 50 nM–1 μM. Initial velocities were obtained at different fixed concentrations of [^{3}H]AdoMet (500 nM and 1, 1.5, and 2 μM). The reaction mixture was incubated for 2.5 min at 37 °C. Similarly, by varying the concentration of [^{3}H]AdoMet in the range of 50 nM–2 μM, other reaction conditions remaining identical, methylation assays were carried out to determine initial velocities. Initial velocities were obtained at various fixed concentration of DNA (250, 500, and 750 nM and 1 μM). The double reciprocal plot allowed determination of the dependence of DNA on AdoMet and vice versa. While determining initial velocities, the product formed was measured under such conditions that overall inhibition of the reaction by AdoHcy was less than 5%.

Product Inhibition Studies—Methylated DNA was obtained for inhibition studies as follows. pUC18 supercoiled plasmid DNA was incubated with *Kpn*I MTase (2 μM) and AdoMet (5 μM) at 37 °C for 1 h. Methylated DNA was extracted twice with phenol-chloroform, precipitated with absolute ethanol, and dried. The concentration of DNA estimated, and the DNA was used. Methylation of DNA was further confirmed by restriction digestion with *Kpn*I endonuclease.

Product inhibition studies were done under identical conditions as described for initial velocity dependence experiments. Inhibition by AdoHcy was studied using 1 μM pUC18 supercoiled plasmid DNA (fixed concentration) while keeping the AdoHcy concentrations fixed (0, 1, 5, and 10 μM) and varying the concentration of [^{3}H]AdoMet from 50 nM to 2 μM for each of the fixed concentrations of AdoHcy. Similarly, another series of identical reactions included 2 μM [^{3}H]AdoMet (fixed concentration); AdoHcy concentrations fixed at 0, 1, 5, and 10 μM and DNA concentration varied in the range of 50 nM–1 μM for each of the fixed concentration of AdoHcy. Double reciprocal plots of initial velocity *versus* [^{3}H]AdoMet or DNA concentrations were obtained at each concentration of the AdoHcy. K_i AdoHcy was determined from these double reciprocal plots of initial velocity *versus* AdoMet concentration followed by secondary plots with their intercepts (data not shown). For inhibition by methylated DNA, the unmethylated DNA concentration was kept constant at 1 μM, and AdoMet concentration was varied in the range of 50 nM–2 μM against each of the chosen methylated DNA concentrations (0, 0.5, 1, and 2 μM). Similarly, another series of identical reactions was performed at a fixed concentration of [^{3}H]AdoMet (2 μM) and varying concentrations of unmethylated DNA ranging from 50 nM to 1 μM against each of the fixed concentrations of methylated DNA (0, 0.5, 1, and 2 μM). Double reciprocal plots were generated from these data, and K_i of methylated DNA was estimated using secondary plots.

Fluorescence Spectroscopy Analysis of KpnI MTase-AdoMet Interaction—Fluorescence emission spectra and fluorescence intensities were measured for *Kpn*I MTase on a Shimadzu, RF 5000 spectrofluorimeter using a 1-cm stirred quartz cuvette at 37 °C. The emission spectra were recorded over a wavelength of 300–400 nm with an excitation wavelength of 280 nm. *Kpn*I MTase was allowed to equilibrate for 2 min in methylation buffer before measurements were made. Small aliquots of cofactor (final concentration 1 μM–100 μM) were added to *Kpn*I MTase (5 μM), and spectra were recorded. The binding of AdoMet to *Kpn*I MTase resulted in quenching of fluorescence. Each spectra recorded was an average of three scans. The fluorescence intensities were plotted against the total AdoMet concentration, and the data were analyzed according to Stern-Volmer and the modified Stern-Volmer equation (32). The Stern-Volmer relationship is represented by,

$$F_0/F = 1 + K_{SV}[Q] \quad \text{(Eq. 1)}$$

where F_0 and F are fluorescent intensities in the absence and presence of cofactor respectively, K_{SV} is the collision Stern-Volmer constant, and Q is the quencher (AdoMet) concentration. In the case where there is a heterogeneous population of fluorophores, the modified Stern-Volmer relationship is used,

$$F_0/(F_0 - F) = 1/\{[Q] \times fa \times K_0\} + 1/f_a \quad \text{(Eq. 2)}$$

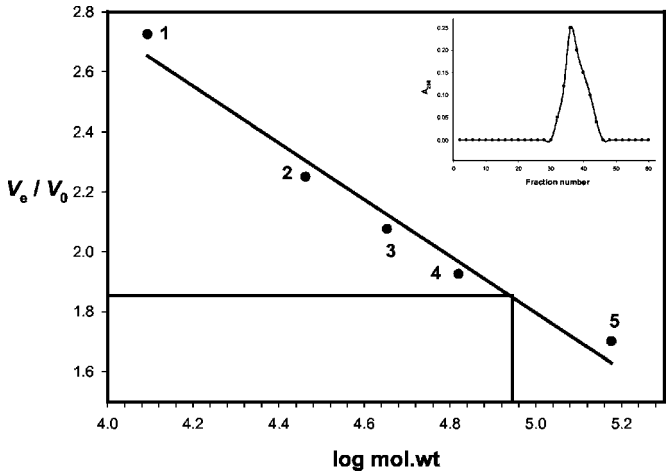

FIG. 2. **Determination of the molecular mass of *Kpn*I MTase by gel filtration chromatography under nondenaturing conditions.** The standard curve V_e/V_o *versus* the log of the molecular weight was derived from the elution profiles of the standard molecular weight markers with V_e corresponding to the peak elution volume of the protein and V_o representing the void volume of the column determined using blue dextran (2,000,000). The peak position of *Kpn*I MTase is indicated by a line. *1*, lysozyme (12.4 kDa); *2*, carbonic anhydrase (29 kDa); *3*, ovalbumin (45 kDa); *4*, bovine serum albumin (66 kDa); *5*, alcohol dehydrogenase (150 kDa). *Inset*, elution profile of *Kpn*I MTase.

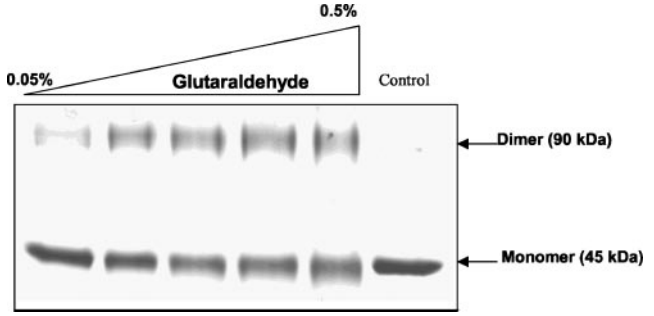

FIG. 3. **Glutaraldehyde cross-linking of *Kpn*I MTase.** *Kpn*I MTase (4.44 μM) was incubated with 0.05%–0.5% of glutaraldehyde (final concentration) at 4 °C for 60 min. Reactions were stopped by adding SDS-loading buffer and boiled for 3 min at 100 °C. The reaction mixtures were analyzed on a 10% polyacrylamide gel containing 0.1% SDS. The gel was silver-stained to visualize the protein. The control lane is *Kpn*I MTase without glutaraldehyde treatment.

where *fa* is the fractional number of fluorophores accessible to the quencher, and K_Q is the quenching constant. The dissociation constants were calculated graphically using the modified Stern-Volmer plot (a plot of $F_0/(F_0 - F)$ *versus* 1/[Q]), where $K_Q = 1/K_d$ (33, 34).

Isotope Partitioning Analysis—*Kpn*I MTase (1 μM) was preincubated with [^{3}H]AdoMet (4 μM) at 37 °C for 5 min. The preincubated reaction mix was brought to a final volume of 150 μl with methylation buffer containing 4 μM [*methyl*-^{3}H]AdoMet and 600 nM DNA. Aliquots of 20 μl each were removed at 10-, 20-, 30-, 40-, 50-, and 60-s time intervals, and the reaction was stopped by snap-chilling the samples in liquid nitrogen. Samples were then analyzed for radiolabeled product formation using a DE81 filter binding assay. In a parallel reaction, the above-mentioned preincubated mix was brought to 150 μl with methylation buffer containing 4 μM unlabeled AdoMet and 600 nM DNA, and the reaction was carried out as described earlier.

DNA Binding Studies; Surface Plasmon Resonance Analysis—The binding kinetics of purified *Kpn*I MTase with DNA was determined by surface plasmon resonance spectroscopy using the BIACORE 2000 optical biosensor (Amersham Biosciences). The 24-mer (duplex XI) with one *Kpn*I recognition sequence containing a 5′-biotinylated oligonucleotide was immobilized on a streptavidin-coated chip (Amersham Biosciences) as per the manufacturer's recommendations. *Kpn*I MTase titration (concentration range, 75–150 nM) was performed in buffer containing 10 mM HEPES, pH 7.4, 25 mM NaCl, 1 mM EDTA, and 0.05% surfactant P-20. The surface was regenerated by passing 5 μl of 0.05% SDS followed by 10 μl of 1 M NaCl for further binding reactions. The

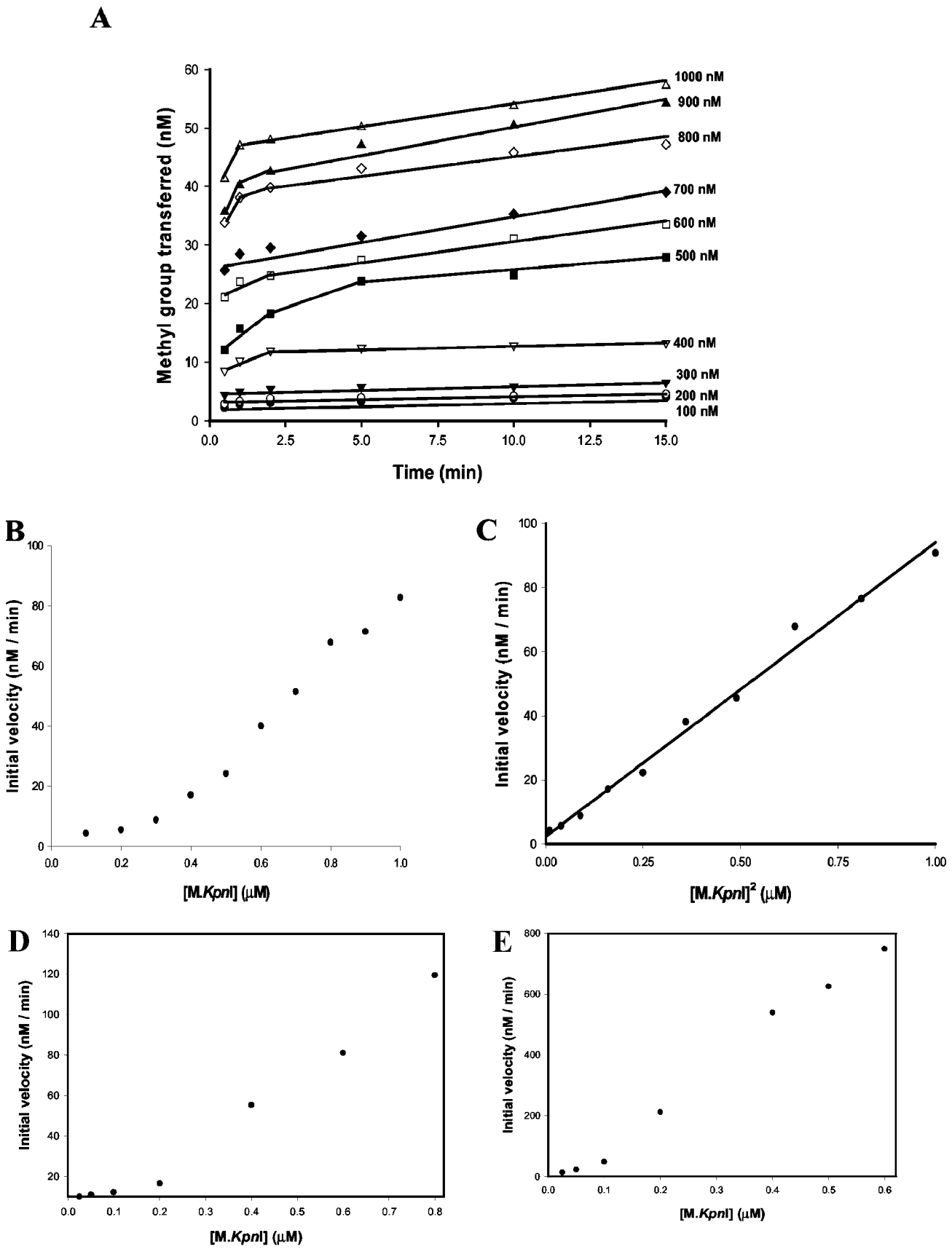

FIG. 4. **Rate of DNA methylation at different *Kpn*I MTase concentrations.** Methylation assays were carried out in a reaction mixture containing 1 μM supercoiled pUC18 plasmid DNA, 2 μM [*methyl*-^{3}H]AdoMet, and 100 nM to 1 μM *Kpn*I MTase in standard reaction buffer at 37 °C. At regular time intervals, the samples were removed and analyzed as described under "Experimental Procedures." *A*, curves obtained from time course methylation assays at different concentrations of *Kpn*I MTase. *B*, initial velocity *versus Kpn*I MTase concentration. *C*, initial velocity *versus* square of *Kpn*I MTase concentration. *D*, initial velocity *versus Kpn*I MTase concentration with unmethylated oligonucleotide (duplex IX). *E*, initial velocity *versus Kpn*I MTase concentration with hemimethylated oligonucleotide (duplex X).

TABLE I
Kinetic parameters of Kpn1 MTase catalyzed methylation of DNA

DNA substrate	K_M DNA	K_MAdoMet	K_{cal}	K_{cal}/K_M DNA
	(μM)	(μM)	(s^{-1})	$M^1\ s^{-1}$
pUC18 supercoiled DNA	0.15	0.56	3.3×10^{-4}	2.2×10^3
pUC18 linear DNA	0.09		7.2×10^{-4}	8.0×10^3
Duplex IX (38-mer) (unmethylated)	1.95	0.65	2.2×10^{-3}	1.1×10^3
Duplex X (38-mer) (hemimethylated)	1.42		5.6×10^{-3}	4.0×10^3

binding data was analyzed using BIA evaluation software (version 3.1). One of the four surfaces was used as a negative control for the interaction.

Data Analysis—Unless otherwise indicated, all enzyme activity data are the average of at least triplicate determinations. Data points were collected in duplicate, plotted as Lineweaver-Burk double reciprocal plots, and fit to weighted linear regressions. The Michaelis-Menten equation was used for all studies described here. The following equations were used.

$$\text{Hyperbola,}\quad v = \frac{V_{max}[S]}{K_m + [S]} \qquad \text{(Eq. 3)}$$

Ordered mechanism,

$$E + A \underset{k_{-1}}{\overset{k_1}{\longleftrightarrow}} EA + B \underset{k_{-2}}{\overset{k_2}{\longleftrightarrow}} EAB \xrightarrow{k_{cat}} E + P + Q \qquad \text{(Eq. 4)}$$

$$v = \frac{V_{max}[A][B]}{K_{ia}K_b + K_b[A] + K_a[B] + [A]} \qquad \text{(Eq. 5)}$$

K_{ia} is the dissociation constant for the EA complex, K_a is the Michaelis constant for A, and K_b is the Michaelis constant for B. Other mechanisms were eliminated by demonstrating unacceptable fits of the data to the appropriate equations.

$$\text{Competitive inhibition,}\quad v = \frac{V_{max}[S]}{K_m(1 + I/K_i) + [S]} \qquad \text{(Eq. 6)}$$

$$\text{Noncompetitive inhibition,}\quad v - \frac{V_{max}[S]}{K_m + [S](1 + I/K_i)} \qquad \text{(Eq. 7)}$$

The parameters are as follows: v, initial velocity; V_{max}, maximum velocity; K_m, Michaelis constant; K_i, inhibition constant.

RESULTS AND DISCUSSION

Preliminary Characterization of KpnI MTase—In the present work, we sought to obtain kinetic insights into events underlying the interaction of enzyme with substrates and their relationship to catalysis. *Kpn*I MTase was purified to homogeneity and purity of the protein judged as being greater than 99% on SDS-polyacrylamide gel electrophoresis. Enzyme preparations used for the kinetic analysis showed an optimal activity at a pH 8.0 and 37 °C in the presence of 100 mM KCl. No product inhibition was observed under initial velocity conditions. Thermal stability experiments showed that *Kpn*I MTase was completely inactive when incubated at 37 °C for 30 min in the absence of substrates.

Molecular Mass Determination—Gel filtration analysis was performed to determine size and subunit structure of *Kpn*I MTase in solution. Superdex 200 column was calibrated with proteins of known size (12–150 kDa), and different concentrations of *Kpn*I MTase were loaded (11.1–222.2 μM). *Kpn*I MTase eluted as a symmetric peak at a position corresponding to a globular protein of ~90 kDa (Fig. 2), suggesting that the enzyme exists as a dimer under native conditions.

Glutaraldehyde is a homobifunctional cross-linking reagent that cross-links N-terminal primary amines of lysine residues, resulting in the formation of amidine cross-links between protein subunits. *Kpn*I MTase contains 36 lysine residues/molecule. Chemical cross-linking of *Kpn*I MTase with glutaraldehyde was carried out to determine the oligomeric nature of the enzyme. Glutaraldehyde-treated *Kpn*I MTase migrated with a relative molecular mass of 90 kDa (Fig. 3). It was observed that increasing the concentration of glutaraldehyde in the cross-linking reaction mixture resulted in an increase in the cross-linked *Kpn*I MTase. These results demonstrate that *Kpn*I MTase exists as a dimer in solution.

Based on the amino acid sequence, the molecular mass of *Kpn*I MTase was calculated to be ~47 kDa. The molecular mass of purified protein determined by SDS-polyacrylamide gel electrophoresis was ~45 kDa. However, size-exclusion chromatography analysis (Fig. 2) and chemical cross-linking by glutaraldehyde (Fig. 3) showed that *Kpn*I MTase exists as a dimer in solution in the concentration range of 11.1–222.2 μM.

Most of the characterized MTases such as *Hha*I MTase (10), *EcoR*I MTase (29), and *Eco*Dam (35) MTase exist as monomers in solution. However, MTases such as *Ccr*M MTase (36), adenine MTases from *Dpn*II R-M systems (37), *EcoP*15I MTase (38), human placental DNA (cytosine-5) methyltransferase (39), and *Hae*IV MTase (40) exist as dimers in solution. *Rsr*I MTase (41) and *Msp*I MTase have been shown to dimerize at high protein concentrations (42).

Rate of Methylation Versus Enzyme Concentration—To establish the relationship between the initial velocity of the reaction and enzyme concentration, the rate of DNA methylation catalyzed at different *Kpn*I MTase concentrations was determined. The substrate used for this analysis was pUC18 plasmid DNA with a single *Kpn*I (GGTACC) site. Varying concentrations (0.1–1 μM final concentration) of *Kpn*I MTase was added to the reaction mixture containing DNA and AdoMet and incubated at 37 °C. The progress of methylation was monitored by withdrawal of 20-μl samples at timed intervals. All time courses displayed a rapid burst in product formation followed by a slower rate of product formation at various *Kpn*I MTase concentrations (Fig. 4*A*). This is consistent with an initial burst in product formation followed by a rate-limiting step after methyl transfer. These curves were further used to calculate the initial velocity ($v_o = d[P]/dt$) of each reaction catalyzed by a given *Kpn*I MTase concentration. When initial velocities were plotted against the corresponding enzyme concentration a nonlinear plot was obtained (Fig. 4*B*). This indicated that, at low concentrations of *Kpn*I MTase, the initial velocity of the reaction is not directly proportional to the enzyme concentration, suggesting that *Kpn*I MTase-catalyzed reaction is higher than first order with respect to enzyme concentration. The nonlinear relationship of enzyme concentration on rate of DNA methylation strongly suggests cooperative binding of two molecules of *Kpn*I MTase to DNA. Furthermore, replotting the initial velocity of the reaction against the square of *Kpn*I MTase concentration yielded a linear plot (Fig. 4*C*). These results indicate that the cooperative binding of two molecules of *Kpn*I MTase is required to methylate DNA.

Similar experiments were carried out using both unmethylated (duplex IX) and hemimethylated oligonucleotides (duplex X) to determine whether *Kpn*I MTase exists as a dimer on these short oligonucleotides. Dependence of initial velocity on enzyme concentration with these oligonucleotides was higher than first order (Fig. 4, *D* and *E*). But the nonlinear relationship of enzyme concentration on the rate of DNA methylation is

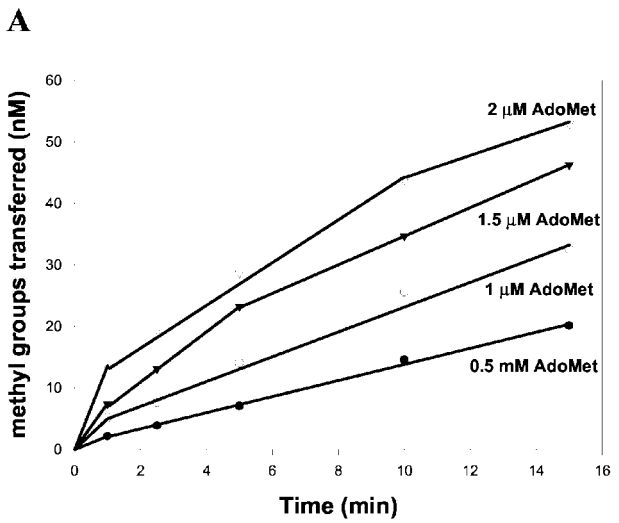

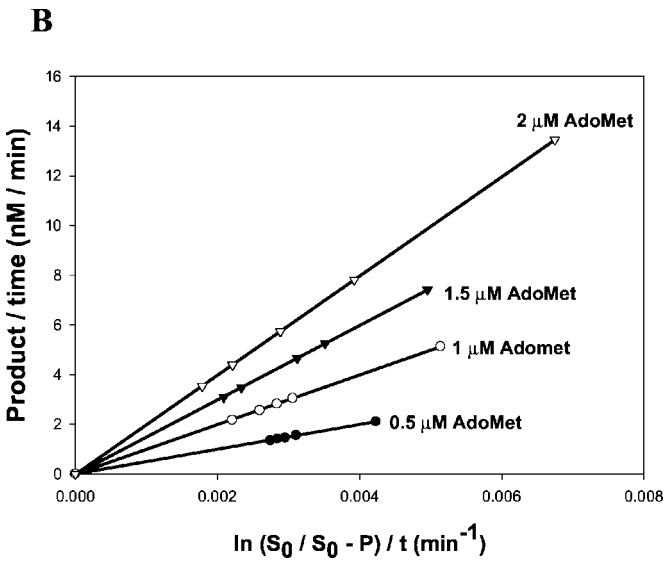

FIG. 5. **Progress curve analysis of the methylation reaction of *Kpn*I MTase.** Time courses of methylation assays were carried out in reactions containing 1 μM pUC18 supercoiled DNA, the indicated concentration of [*methyl*-^{3}H]AdoMet, and 1 μM *Kpn*I MTase under standard conditions. Samples were withdrawn at the time intervals indicated and analyzed as described under "Experimental Procedures." The data shown in *A* were fitted to Equation 8, and the data obtained were plotted as shown in *B*.

much less pronounced with hemimethylated oligonucleotide than what was observed when plasmid DNA and unmethylated oligonucleotide were used.

It is clear from the data shown above that *Kpn*I MTase exists as a dimer in solution and during methylation of its recognition sequence, unlike almost all other MTases belonging to type II R-M system. The significance of the dimeric nature of *Kpn*I MTase in solution and upon interaction with DNA is not clear at the present time. We have considered the possibility that dimeric enzymes have higher affinity for DNA and may be more proficient. But the results presented below do not reflect this behavior in the case of *Kpn*I MTase, which is clear from the kinetic parameters determined (Table I and see Fig. 12). An

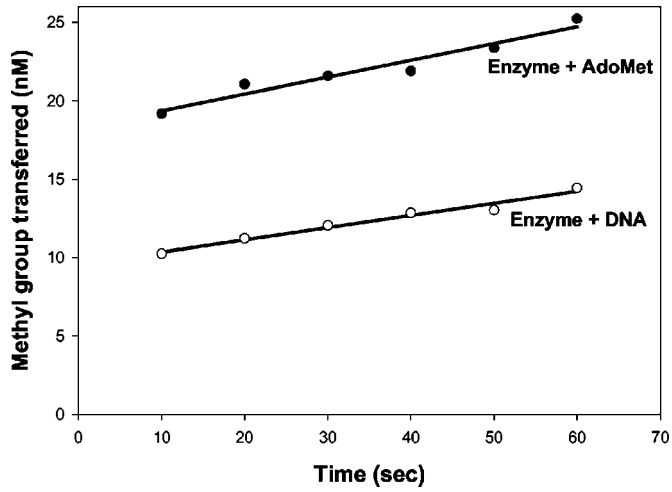

FIG. 6. **Preincubation analysis of *Kpn*I MTase.** Methylation reactions were carried out in methylation buffer containing 1 μM *Kpn*I MTase, 1 μM pUC18 supercoiled DNA, and 2 μM [*methyl*-^{3}H]AdoMet. Methylation reactions were started by the addition of DNA to a solution containing enzyme and AdoMet (●) or by the addition of AdoMet to a solution containing enzyme and DNA (○).

alternative possibility is that *Kpn*I MTase originated from an ancestral dimeric MTase. The amino acid sequence of *Kpn*I MTase has maximum homology with the amino acid sequence of the members of type III R-M systems (7). It is tempting to speculate that *Kpn*I MTase might have derived from MTases belonging to type III R-M systems.

Progress Curve Analysis of Methylation Reaction—Time courses of methylation by *Kpn*I MTase at various concentrations of AdoMet were carried out to determine the period during which the rate of product formation remains linear. A plot of methyl groups transferred *versus* time was obtained (Fig. 5*A*). *Kpn*I MTase-catalyzed rate of methylation decreased progressively with increasing AdoMet concentrations. The decrease in rate was inversely proportional to the AdoMet concentration. The inhibition appears to be competitive with respect to AdoMet due to the formation of AdoHcy or methylated DNA, and the nonlinear kinetics are consistent with competition by AdoHcy generated in the reaction (see later in this section of text). This behavior was not because of enzyme degradation under these conditions (data not shown).

The progress curves shown in Fig. 5*A* fit in Equation 8, which describes a reaction wherein the product, AdoHcy in this case, competes with substrate, AdoMet,

$$P/t = \frac{V_{max}}{1 - (K_M/K_i)} + \frac{K_M(K_i + S_0) \times 1/t}{K_M - K_i} \times \frac{\ln S_0}{S_0 - P} \qquad \text{(Eq. 8)}$$

where P is the amount of AdoHcy formed at time t, S_0 is the initial AdoMet concentration, and K_i is the dissociation constant of AdoHcy. The amount of AdoHcy formed corresponds to the amount of methylated DNA, the product that is measured in these experiments. A plot of P/t *versus* $\ln S_0/(S_0 - P)/t$ provides a series of lines with positive slopes converging on the negative side on the ordinate (Fig. 5*B*).

Preincubation Studies with KpnI MTase—For the catalytic cycle of DNA MTases, binding of substrates could occur in a random or sequential order. To determine this, *Kpn*I MTase was preincubated with [*methyl*-^{3}H]AdoMet or with pUC18 DNA for 5 min, and the reaction was initiated by adding DNA or [*methyl*-^{3}H]AdoMet, respectively. Under saturating substrate conditions, the order of preincubation of *Kpn*I MTase with AdoMet and DNA had significant influence on the rate of product formation. As seen in Fig. 6, the preformed enzyme-DNA complex is slightly less efficient than the preformed en-

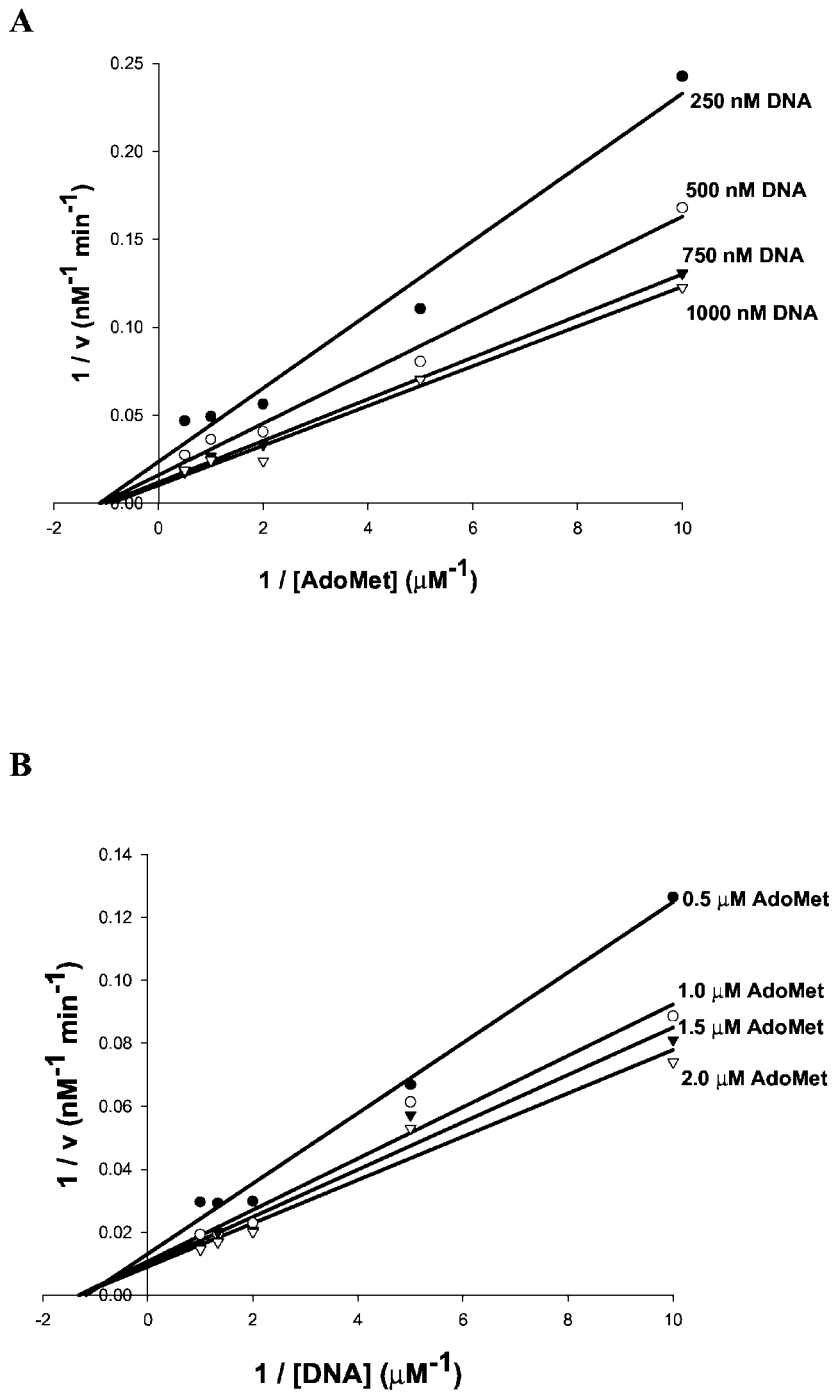

FIG. 7. **Double reciprocal plots of the initial velocity *versus* substrate concentration.** Reactions contained the indicated concentrations of pUC18 plasmid DNA and [*methyl*-^{3}H]AdoMet in standard buffer at 37 °C. *Kpn*I MTase (1 μM final concentration) was added to start the reaction. The samples were withdrawn at 2.5-min intervals and assayed as described under "Experimental Procedures." *A*, double reciprocal plots of the rates of methylation *versus* AdoMet concentrations at different fixed concentrations of DNA. *B*, double reciprocal plots of the rates of methylation *versus* DNA concentrations at different fixed concentrations of AdoMet.

zyme-AdoMet complex in methylating DNA. Preincubation studies with unmethylated oligonucleotides (duplex IX) produced similar results (data not shown).

From preincubation experiments it appears that the enzyme may have a random order of substrate binding; the route via the enzyme-AdoMet complex is kinetically more efficient than via the enzyme-DNA complex. One explanation for this would be that the preformed enzyme-DNA complex is not catalytically competent and that it must dissociate, bind AdoMet, and then rebind DNA, which could slow down productive complex formation. Therefore, although preincubation studies suggest that either substrate could bind enzyme, it is evident from initial velocity experiments and product inhibition studies (see below in this section) that *Kpn*I MTase obeys an ordered mechanism in which AdoMet binds first, followed by DNA. A similar study performed with *Eco*RV MTase clearly showed differences in product formation. Under the preincubation conditions, *Eco*RV MTase-DNA complex was not active, whereas enzyme-AdoMet complex was active (25). In the case of T4 Dam, the preformed T4 Dam-AdoMet complex was catalytically more efficient than the preformed T4 Dam-DNA complex during the first round of catalysis, and this is consistent with the order of binding where AdoMet binds first (43).

Determination of Kinetic Parameters—To determine initial velocities, product formation was measured under conditions such that maximal final concentration of AdoHcy generated in the reactions was less than 1 nM. These constraints ensured that the overall inhibition of the reaction by AdoHcy was less than 5%.

Using double reciprocal plots of initial velocity *versus* substrate concentration, the kinetic parameters (K_m^{DNA}, K_m^{AdoMet}, and $V_{\max}$) were calculated. The catalytic constant, k_{cat}, was obtained as the ratio of maximal velocity to enzyme concentra-

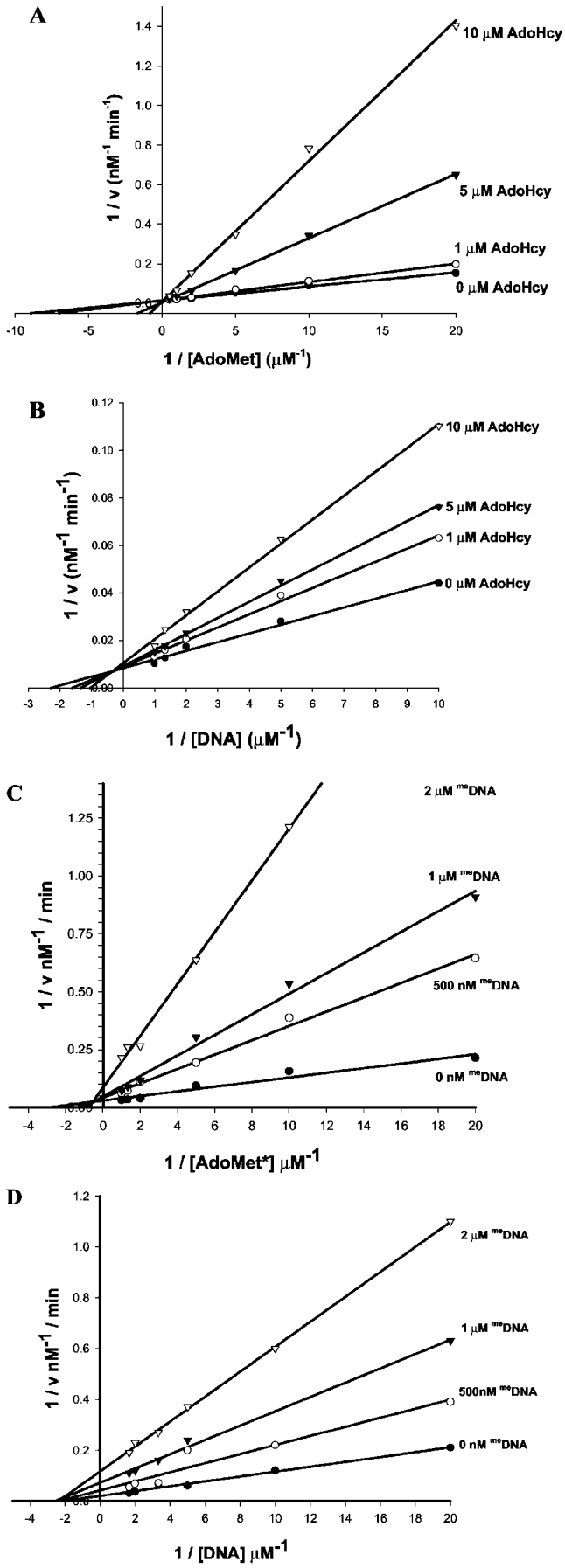

FIG. 8. **Product inhibition analysis of methylation catalyzed by *Kpn*I MTase.** The reactions contained the indicated concentrations of pUC18 DNA, [*methyl*-^{3}H]AdoMet, AdoHcy, and methylated DNA in standard reaction buffer at 37 °C. *Kpn*I MTase was added to a final concentration of 1 μM. The samples were withdrawn at regular time intervals and assayed as described under "Experimental Procedures." *A*, double reciprocal plots of the rates of methylation *versus* AdoMet concentrations at different fixed concentrations of AdoHcy. *B*, double reciprocal plots of rates of methylation *versus* DNA concentrations at different fixed concentrations of AdoHcy. *C*, double reciprocal plots of rates of methylation *versus* AdoMet concentrations at different fixed concentrations of methylated DNA. *D*, double reciprocal plots of rates of methylation *versus* DNA concentrations at different fixed concentrations of methylated DNA.

tion. The specificity constant was determined as k_{cat}/K_m^{DNA}. In all these assays, the substrate used was pUC18 plasmid DNA with a single *Kpn*I recognition sequence. Values for all the kinetic parameters for different DNA substrates and AdoMet have been listed in Table I. The k_{cat} of *Kpn*I MTase with plasmid DNA obtained is 3.3×10^{-4} s^{-1}, whereas the measured k_{cat} values for other MTases were 5.3×10^{-3} s^{-1} for *Eco*P15I (44), 3.4×10^{-3} s^{-1} for *Eca*I (22), 0.175 s^{-1} for *Bam*HI (45), 2.2×10^{-2} s^{-1} for *Hha*I (10), 0.124 s^{-1} for *Eco*RI (19), 4.2×10^{-5} s^{-1} for DNMT1, and 7.2×10^{-6} s^{-1} for DNMT3a (17). The k_{cat} value obtained with duplex X (hemimethylated) (5.6×10^{-3} s^{-1}) was 2.5-fold more than the k_{cat} value obtained with duplex IX (unmethylated) (1.1×10^{-3} s^{-1}). This is consistent with hemimethylated DNA being a preferable substrate for DNA MTases *in vivo*. DNMT1 has been shown to have a 7–21-fold preference for hemimethylated DNA than unmethylated DNA. However, DNMT3a preferred unmethylated DNA more than 3-fold over hemimethylated DNA (17). *Rsr*I MTase has a 2–3-fold higher affinity for hemimethylated DNA than unmethylated DNA (21), unlike *Eco*RI MTase, which displays no binding preference between unmethylated and hemimethylated DNA (46). *Kpn*I MTase showed higher affinity to linear plasmid DNA than to supercoiled DNA. *Kpn*I MTase showed lesser affinity toward oligonucleotide compared with longer DNA substrates (Table I). *Kpn*I MTase methylated hemimethylated oligonucleotide (duplex X) more efficiently with higher affinity than unmethylated oligonucleotide (duplex IX). The specificity constant for plasmid DNA (2.2×10^3 m^{-1}s^{-1}) was 3.6-fold lesser than linear DNA (8.0×10^3 m^{-1}s^{-1}). In the case of hemimethylated oligonucleotide, k_{cat}/K_m was 4-fold higher than unmethylated oligonucleotide. *Kpn*I MTase did not methylate single-stranded oligonucleotides (data not shown). All of the DNA MTases that have been characterized kinetically display very slow turnover or rate of methylation. The low turnover coupled with strong binding to their DNA target sequence, as determined by K_m, means that k_{cat}/K_m is high and that the MTases show fair to high specificity for methylation of their target sequence.

Initial Velocity Studies with DNA and AdoMet—The effect of different concentrations of DNA and AdoMet on the initial velocity was determined by the initial velocity dependence studies (Fig. 7). Initial velocity experiments provide clues to differentiate between ordered and ping-pong mechanisms. These experiments were carried out at various concentrations of [^{3}H]AdoMet and pUC18 plasmid DNA. The double reciprocal plots of 1/*v* *versus* 1/[DNA] (Fig. 7*A*) and 1/*v* *versus* 1/[AdoMet] (Fig. 7*B*) gave a series of lines intersecting on the left side of the 1/*v* axis that are characteristic patterns for a ternary complex formation. The transformed data were best fitted by lines intersecting at quadrant IV. These results suggest that methylation proceeds by a random or ordered bi bi mechanism. The fact that double reciprocal plots (1/*v* *versus* 1/[S]) show linear dependence imply that a random mechanism can be ruled out. A ping-pong mechanism is also ruled out, because the lines are not parallel.

Product Inhibition Kinetics—Product inhibition studies with AdoHcy and methylated DNA were carried out to distinguish between ordered and random mechanisms. Product inhibition

TABLE II
Product inhibition of KpnI MTase

^{Me}DNA, methylated DNA.

Product	Variable substrate	Fixed substrate	Type of Inhibition	Inhibition constant
AdoHcy	AdoMet	DNA	Competitive	0.62 μM
AdoHcy	DNA	AdoMet	Noncompetitive	5.60 μM
^{Me}DNA	AdoMet	DNA	Mixed	0.30 μM
^{Me}DNA	DNA	AdoMet	Noncompetitive	0.40 μM

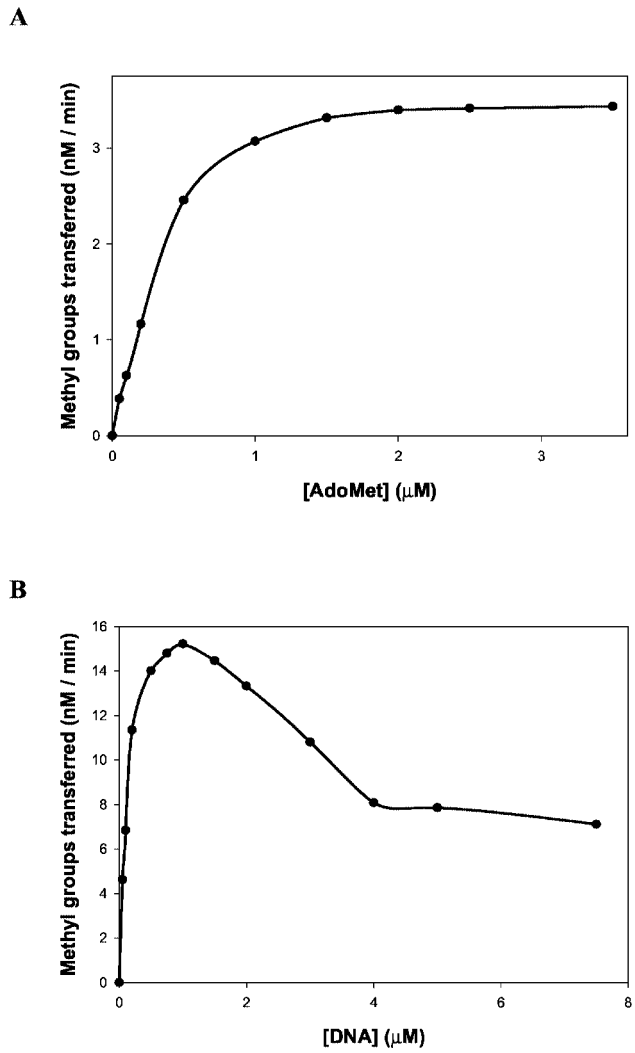

FIG. 9. **Substrate inhibition analysis of *Kpn*I MTase.** *A*, each reaction contained 1 μM *Kpn*I MTase, 1 μM pUC18 supercoiled DNA, and varying concentrations of AdoMet (0.05–3.5 μM). *B*, *Kpn*I MTase concentration was fixed at 1 μM, and AdoMet concentration was fixed at 2 μM. DNA concentration was varied from 0.05 to 7.5 μM. Reaction mixtures were incubated for 2.5 min, and product was estimated as described under "Experimental Procedures."

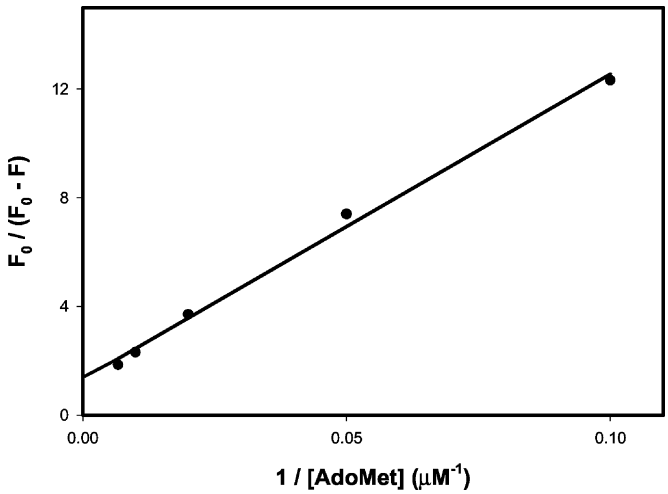

FIG. 10. **Modified Stern-Volmer plot for AdoMet quenching.** Fluorescence experiments were performed at an enzyme concentration of 1 μM at 37 °C in methylation buffer. An excitation wavelength of 280 nm and emission spectra from 300–400 nm were recorded. Fluorescence changes were calculated from the intensity of the maximal intensity of enzyme alone (before addition of cofactor), F_0, and the maximal intensity after the addition of AdoMet, F (10–200 μM).

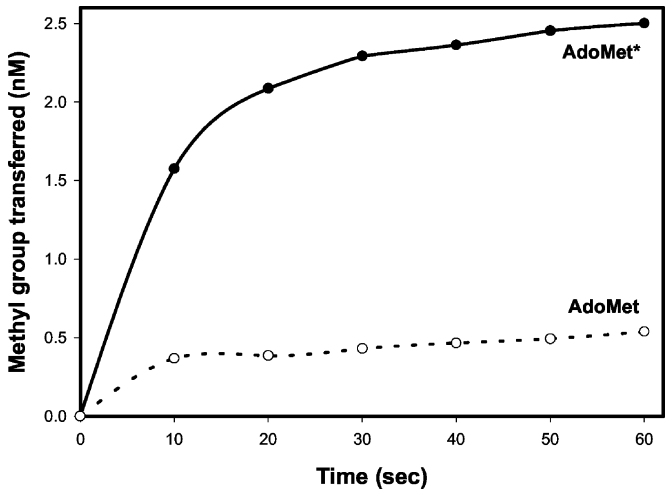

FIG. 11. **Isotope partitioning analysis of *Kpn*I MTase.** Methylation assays were carried out in reaction mixtures containing 1 μM *Kpn*I MTase, 600 nM DNA, and 4 μM AdoMet. Curve 1 (●), product formation after enzyme was preincubated at 37 °C with high specific activity [*methyl*-^{3}H]AdoMet (78.9 Ci/mmol), and the reaction was started with DNA and labeled [*methyl*-^{3}H]AdoMet. Curve 2 (○), product formation after enzyme was preincubated with high specific activity [*methyl*-^{3}H]AdoMet, and the reaction was started with DNA and unlabeled AdoMet.

is examined by the slopes and *y* axis intercepts from families of double reciprocal plots. One substrate is held constant, whereas one product and the other substrate being studied are varied in a concentration range around its Michaelis constant. Inhibition profiles are characterized as competitive, noncompetitive, or uncompetitive. The inhibition constants are derived from analysis of the intercept and slope effects in secondary plots. Ordered mechanisms give competitive patterns with the first substrate that binds to the enzyme *versus* the last product that leaves the enzyme and noncompetitive patterns with any other combinations. AdoHcy was a competitive inhibitor of AdoMet (Fig. 8*A*). The competitive nature of AdoMet with respect to AdoMet binding (K_i = 0.62 μM) suggested that AdoMet and AdoHcy bind to the same form of the enzyme. The AdoHcy inhibition with respect to varying DNA concentrations yielded a series of lines intersecting on the left side of the *x* axis and is, therefore, a noncompetitive inhibitor with respect to DNA (Fig. 8*B*).

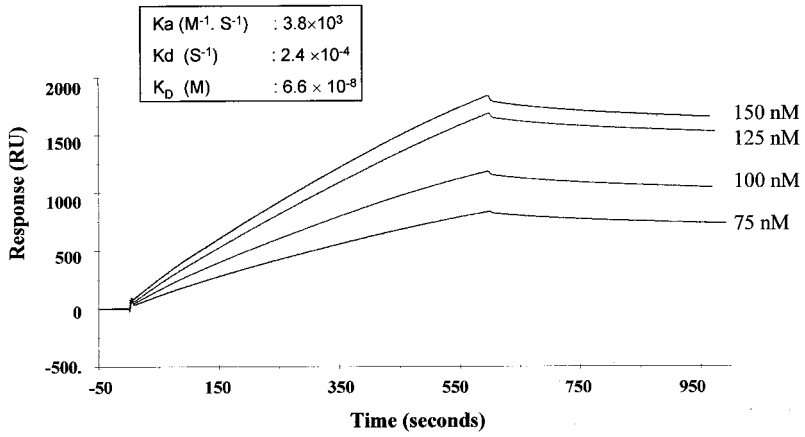

FIG. 12. **Interaction of *Kpn*I MTase at the recognition sequence by surface plasmon resonance.** Shown is a sensogram displaying the response of increasing *Kpn*I MTase concentration (75–150 nM). *Kpn*I MTase was injected for 300 s over streptavidin chips containing immobilized cognate DNA at flow rate of 10 μl/min followed by a dissociation phase of 300 s.

To distinguish between ordered and random mechanisms and to characterize the order of substrate binding, we determined the inhibition pattern with methylated DNA and DNA at saturating AdoMet concentrations. The double reciprocal plot of initial velocity *versus* varying concentrations of AdoMet with respect to different fixed concentrations of methylated DNA yielded a series of lines intersecting just above the left side of the *x* axis (Fig. 8*C*). Therefore, the methylated DNA inhibition is noncompetitive with respect to varying AdoMet as a substrate. Because the double reciprocal plot of initial velocity *versus* concentrations of DNA yielded a series of lines intersecting at *x* axis, methylated DNA was noncompetitive with DNA when AdoMet was held constant (Fig. 8*D*). The observed noncompetitive pattern is inconsistent with any ordered mechanism in which DNA is required to bind first. A random bi-bi order of substrate addition and product release should produce a series of four product inhibition plots that are all noncompetitive. Hence, the patterns in Fig. 8 are inconsistent with a random bi-bi mechanism. Consistent with the observed pattern is an AdoMet binding first, ordered steady state mechanism. The data obtained from *Kpn*I MTase product inhibition studies are summarized in Table II.

In the case of *Eco*RI MTase (19–20), *Eco*RV MTase (25), and T4 Dam (26), the reaction mechanism is ordered with AdoMet binding first to the enzyme, which is similar to the proposed reaction mechanism for *Kpn*I MTase. In the case of *Taq*I MTase (24), *Eca*I MTase (22), human DNMT1 (47), and *Eco*P15I MTase (18), the order of substrate binding is random, and in the case of *Hha*I MTase (10), *Msp*I MTase (15), murine C^5 cytosine methyltransferase (14), and mammalian DNMT3a (17), the order of substrate binding is just the reverse, *i.e.* DNA binds first followed by AdoMet. It is noteworthy to mention that DNA MTases in which DNA has been shown to bind first act processively during methylation of specific DNA sequences (10, 47, 23), whereas other DNA MTases in which AdoMet has been shown to bind first methylate in a distributive manner (25, 48).

Substrate Inhibition Studies—To further confirm that the binding of substrates follows an ordered mechanism, studies at high substrate concentrations were carried out. This is also known as substrate inhibition. This analysis has been successfully used to determine the order of binding of substrates in the case of *Eco*P15I MTase (18), T4 Dam (26), and mammalian DNMT3a (17). In a compulsory ordered mechanism, if the initial concentration of the second substrate is sufficiently high, an inhibitory effect on the enzyme would be observed due to the formation of nonproductive binary and/or dead-end ternary complexes. On the contrary, the first substrate to bind does not have an inhibitory effect even at higher concentrations, because the binary complex is catalytically active, and a dead-end complex is not formed. No substrate inhibition is observed in a random mechanism unless a dead end ternary complex is formed. This is because neither of the two binary complexes (Enzyme-AdoMet or Enzyme-DNA) can prevent a productive ternary complex formation. When substrate inhibition studies were carried out with *Kpn*I MTase, no substrate inhibition was observed at AdoMet concentration of up to 3.5 μM (Fig. 9*A*). On the other hand, an inhibition of *Kpn*I MTase was observed by DNA at high concentrations, above 1 μM (Fig. 9*B*). When this experiment was carried out at a lower enzyme concentration, a similar pattern was observed (data not shown). These results suggest that *Kpn*I MTase follows an ordered bi bi mechanism, where AdoMet is the first substrate to bind followed by the binding of DNA. These data are consistent with the results obtained from product inhibition studies.

Our assignment of the kinetic mechanism rests on the following lines of evidence. (*a*) Double reciprocal plots of initial velocity data with AdoMet as the variable substrate and DNA as the fixed substrate and vice versa gave lines of intersecting pattern, which is characteristic of ternary complex formation. These results rule out the random as well as the ping-pong mechanism. (*b*) Product inhibition studies demonstrate that AdoHcy is a competitive inhibitor with respect to AdoMet in methylation reaction (K_i = 0.62 μM) and, therefore, binds to the free enzyme form. (*c*) Inhibition studies with methylated DNA demonstrate that it binds to the enzyme-AdoMet binary complex. Noncompetitive inhibition demonstrates the formation of both an enzyme-DNA and enzyme-AdoMet complex. (*d*) Substrate inhibition studies showed that at higher concentrations of DNA, the inhibition was severe, but AdoMet did not show inhibition even at higher concentrations.

Isotope Partitioning Studies—Isotope partitioning analysis of *Kpn*I MTase was carried out to examine the competency of *Kpn*I MTase-AdoMet complex. First, we determined the K_D for AdoMet by fluorescence-quenching experiments. The intrinsic fluorescent properties of *Kpn*I MTase were exploited in a fluorescence-quenching assay to determine the dissociation constant for AdoMet. The Stern-Volmer plot (49) and modified Stern-Volmer plot (32) were used to analyze the quenching data. The Stern-Volmer plot for AdoMet showed a negative deviation from linearity, a result expected only when a fraction of the tryptophans are accessible to quenching by ligand binding (data not shown). Therefore, a modified Stern-Volmer plot was used to analyze the quenching. The data in Fig. 10 gave a linear plot. This linearity suggests that cofactor binding is the dominant fluorescence-quenching phenomenon over the range of concentrations checked (1–100 μM). The K_D value calculated from modified Stern-Volmer relationship (Equation 2) was 4 μM.

AdoMet concentrations were chosen based on the K_D^{AdoMet} determined from the fluorescence-quenching experiments. In

an isotope partitioning experiment, a presaturated binary complex of *Kpn*I MTase with [^{3}H]AdoMet was diluted into a mixture containing excess DNA and unlabeled AdoMet to determine what fraction of the bound-labeled AdoMet would react before exchanging with unlabeled cofactor. The formation of radiolabeled product reflects the propensity of the enzyme-bound labeled substrate to undergo catalysis without dissociation (50). Preincubation of *Kpn*I MTase with [^{3}H]AdoMet (4 μM) results in a burst of product formation upon the addition of DNA and labeled AdoMet (Fig. 11, ●). The burst was followed by a constant rate of product formation. A decreased burst was observed when unlabeled AdoMet was used in the chase (Fig. 11, ○). However, this burst was much smaller in size than that observed in the first case. Burst magnitude is defined as the vertical axis intercept resulting from extrapolation of the linear portion of the progress curve to zero time. These results indicate that the *Kpn*I MTase-AdoMet complex formed is catalytically competent. This is so because a chase including 600 nM DNA and 4 μM unlabeled AdoMet produced detectable activity. The detection of a burst in the isotope-partitioning assay also provides evidence that the prebound AdoMet is catalytically competent and supports an ordered bi bi mechanism wherein AdoMet binds first. If DNA were required to bind to *Kpn*I MTase before AdoMet for catalysis, all of the prebound AdoMet would form catalytically nonproductive complex. These results further support the kinetic mechanism as steady state rather than rapid equilibrium.

Isotope partitioning technique has been used successfully to determine the catalytic competency of enzyme substrate complex and to decipher the order of binding in *Eco*RI MTase (19), *Hha*I MTase (12, 13, 51) *Msp*I MTase (15), the murine DNA (cytosine) MTase (14), and *Rsr*I MTase (21). The requirement of DNA binding for the formation of competent complex was found in the case of murine DNA (cytosine) MTase (14), whereas for *Eco*RI MTase (19), *Hha*I MTase (13), and *Rsr*I MTase (21) the enzyme-AdoMet complex was found to be catalytically active.

Methylation Assays with Noncanonical Oligonucleotides—The recognition sequence of the *Kpn*I R-M system is 5′-GGTACC-3′, and *Kpn*I endonuclease cleaves within this sequence. *Kpn*I endonuclease is also known for its star activity as it cleaves DNA at nonspecific sequences.[2] We were, therefore, interested to find out if *Kpn*I MTase would methylate oligonucleotides containing noncanonical sequences. Methylation assays were carried out with seven different oligonucleotides containing noncanonical sequences (duplexes I-VII) with one base change in the recognition sequence and an oligonucleotide (duplex VIII) containing *Kpn*I recognition sequence (data not shown). These assays showed no significant methylation at nonspecific sites by *Kpn*I MTase even when enzyme was used in far excess and the enzyme methylated only at its specific recognition sequence (data not shown).

Kinetics of DNA Binding—Surface plasmon resonance spectroscopy was used to determine the kinetics of DNA binding for *Kpn*I MTase. Surface plasmon resonance measures change in the refractive angle arising from a binding event. Experiments focusing on DNA-protein interactions require the DNA to be immobilized on the surface of the flow cell and the enzyme under study to be passed over the surface in increasing concentrations to allow determination of binding constants. The association and dissociation of the protein to DNA was monitored by changes in the refractive index due to the binding event on the sensor surface. To determine *Kpn*I MTase-DNA stoichiometry, a DNA substrate was synthesized that contained a 3′-biotin tag (duplex XI), which was immobilized through a biotin-streptavidin interaction on the surface of a streptavidin chip. The background nonspecific binding and bulk concentration of *Kpn*I MTase were experimentally determined by simultaneous injection over a surface that lacked DNA. These results demonstrate that *Kpn*I MTase binds to oligonucleotide containing the recognition sequence with high affinity ($K_D = 6.57 \times 10^{-8}$ M) (Fig. 12). The K_d values for other MTase-DNA binary complexes are 10 nM for *Hha*I (13), 17.5 nM for *Rsr*I (21), and 76.9 nM for *Ccr*M (36). It has been shown that the addition of AdoMet or its analogs increases the specificity of several MTases to their recognition sequences (3, 52). However, the addition of cofactor, AdoHcy, did not seem to influence the binding characteristics (data not shown). DNA binding studies and the interaction of cofactor have also been studied using surface plasmon resonance spectroscopy in the case of *Ccr*M (36) and *Eco*R124I (53).

The key finding of the present study is the identification of dimeric nature of *Kpn*I MTase in solution and that it functions as a dimer during methylation reaction. Initial velocity dependence experiments, product inhibition, and substrate inhibition studies demonstrate an ordered mechanism for *Kpn*I MTase where AdoMet binds first followed by DNA. Isotope partitioning analysis showed that the preformed *Kpn*I MTase-AdoMet complex is catalytically competent.

Acknowledgments—We thank Umesh Sankpal for help and useful discussions and S. Arathi for technical assistance.

[2] S. Chandrashekaran and V. Nagaraja, unpublished results.

REFERENCES

1. Wilson, G. G. (1991) *Nucleic Acids Res.* **19,** 2539–2566
2. Ahmad, I., and Rao, D. N. (1996) *Crit. Rev. Biochem. Mol. Biol.* **31,** 361–380
3. Dryden, D. T. F. (1999) in *S-Adenosylmethionine-dependent Methyltransferases: Structure and Functions* (Cheng, X., and Blumenthal, R. M., eds) pp. 283–340, World Scientific Publishing, Singapore
4. Roberts, R. J. (1990) *Nucleic Acids Res.* **18,** 2331–2365
5. Sook Lee, N., Rutebuka, O., Arakawa, T., Bickle, T. A., and Ryu, J. (1997) *J. Mol. Biol.* **271,** 342–348
6. Valinluck, B., Sook Lee, N., and Ryu, J. (1995) *Gene* **167,** 59–62
7. Chatterjee, D. K., Hammond, A. W., Blakesley, R. W., Adams, S. M., and Gerard, G. F. (1991) *Nucleic Acids Res.* **19,** 6505–6509
8. Hammond, A. W., Gerard, G. F., and Chatterjee, D. K. (1990) *Gene* **97,** 97–102
9. Kiss, A., Finta, C., and Venetianer, P. (1991) *Nucleic Acids Res.* **19,** 3460
10. Wu, J. C., and Santi, D. V. (1987) *J. Biol. Chem.* **262,** 4778–4786
11. O'Gara, M., Zhang, X., Roberts, R. J., and Cheng, X. (1999) *J. Mol. Biol.* **287,** 201–209
12. Lindstrom, W. M., Flynn, J., and Reich, N. O. (2000) *J. Biol. Chem.* **275,** 4912–4919
13. Vilkaitis, G., Merkiene, E., Serva, S., Weinhold, E., and Klimasauskas, S. (2001) *J. Biol. Chem.* **276,** 20924–20934
14. Flynn, J., and Reich, N. O. (1998) *Biochemistry,* **37,** 15162–15169
15. Bhattacharya, S. K., and Dubey, A. K. (1999) *J. Biol. Chem.* **274,** 14743–14749
16. Bacolla, A., Pradhan, S., Roberts, R. J., and Wells, R. D. (1999) *J. Biol. Chem.* **274,** 33011–33019
17. Yokochi, T., and Robertson, K. D. (2002) *J. Biol. Chem.* **277,** 11735–11745
18. Rao, D. N., Page, M. G., and Bickle, T. A. (1989) *J. Mol. Biol.* **209,** 599–606
19. Reich, N. O., and Mashhoon, N. (1991) *Biochemistry* **30,** 2933–2939
20. Reich, N. O., and Mashhoon, N. (1993) *J. Biol. Chem.* **268,** 9191–9193
21. Szegedi, S. S., Reich, N. O., and Gumport, R. I. (2000) *Nucleic Acids Res.* **28,** 3962–3971
22. Szilak, L., Der, A., Deak, F., and Venetianer, P. (1993) *Eur. J. Biochem.* **218,** 727–733
23. Berdis, A. J., Lee, I., Coward, J. K., Stephens, C., Wright, R., Shapiro, L., and Benkovic, S. J. (1998) *Proc. Natl. Acad. Sci. U. S. A.* **95,** 2874–2879
24. Wolke, J. (1998) *The Kinetic Mechanism of the DNA Methyltransferase from Thermus aquaticus and Selection of a DNA-binding Peptide by Means of Phage Display.* Ph.D. thesis, University Dortmund, Germany
25. Gowher, H., and Jeltsch, A. (2000) *J. Mol. Biol.* **303,** 93–110
26. Evdokimov, A. A., Zinoviev, V. V., Malygin, E. G., Schlagman, S. L., and Hattman, S. (2002) *J. Biol. Chem.* **277,** 279–286
27. Chandrashekaran, S., Babu, P., and Nagaraja, V. (1999) *J. Biosci.* **24,** 269–277
28. Bradford, M. M. (1976) *Anal. Biochem.* **72,** 248–254
29. Rubin, R. A., and Modrich, P. (1977) *J. Biol. Chem.* **252,** 7265–7272
30. Segel, I. H. (1975) *Biochemical Calculations*, 2nd Ed., pp. 208, John Wiley & Sons, Inc., New York
31. Cornish-Bowden, A. (1995) *Fundamentals of Enzyme Kinetics,* pp. 19, Portland Press Ltd., London
32. Lehrer, S. S. (1971) *Biochemistry,* **17,** 3254–3263
33. Lakowicz, J. R. (1983) *Principles of Fluorescence Spectroscopy*, pp. 259, Plenum Press, New York
34. Samworth, C. M., DegliEsposti, M., and Lenaz, G. (1988) *Eur. J. Biochem.* **171,** 81–86
35. Herman, G. E., and Modrich, P. (1982) *J. Biol. Chem.* **257,** 2605–2612
36. Shier, V. K., Hancey, C. J., and Benkovic, S. J. (2001) *J. Biol. Chem.* **276,**

14744–14751
37. de la Campa, A. G., Kale, P., Springhorn, S. S., and Lacks, S. A. (1987) *J. Mol. Biol.* **196,** 457–469
38. Ahmad, I., Krishnamurthy, V., and Rao, D. N. (1995) *Gene* **157,** 151–155
39. Yoo, H. Y., Noshari, J., and Lapeyre, J. N. (1987) *J. Biol. Chem.* **262,** 8066–8070
40. Piekarowicz, A., Golaszewska, M., Olubumni Sunday, A., Siwinska, M., and Stein, D. C. (1999) *J. Mol. Biol.* **293,** 1055–1065
41. Kaszubska, W., Webb, H. K., and Gumport, R. I. (1992) *Gene* **118,** 5–11
42. Dubey, A. K., Mollet, B., and Roberts, R. J. (1992) *Nucleic Acids Res.* **20,** 1579–1585
43. Malygin, E. G., Lindstrom, W. M., Jr., Schlagman, S. L., Hattman, S., and Reich, N. O. (2000) *Nucleic Acids Res.* **28,** 4207–4211
44. Ahmad, I., and Rao, D. N. (1994) *J. Mol. Biol.* **242,** 378–388
45. Kang, Y. K., Lee, H. B., Noh, M., Cho, N. Y., and Yoo, O. J. (1995) *Biochem. Biophys. Res. Commun.* **206,** 997–1002
46. Reich, N. O., Olsen, C., Osti, F., and Murphy, J. (1992) *J. Biol. Chem.* **267,** 15802–15807
47. Bacolla, A., Pradhan, S., Larson, J. E., Roberts, R. J., and Wells, R. D. (2001) *J. Biol. Chem.* **276,** 18605–18613
48. Surby, M. A., and Reich, N. O. (1996) *Biochemistry* **35,** 2209–2217
49. Stern, O., and Volmer, M. (1919) *Phys. Z.* **20,** 183–188
50. Rose, I. A. (1980) *Adv. Enzymol. Relat. Areas Mol. Biol.* **64,** 47–59
51. Swaminathan, C. P., Sankpal, U. T., Rao, D. N., and Surolia, A. (2002) *J. Biol. Chem.* **277,** 4042–4049
52. Baldwin, G. S., Kelly, S. M., Price, N. C., Wilson, G. W., Connolly, B. A., Artymiuk, P. J., and Hornby, D. P. (1994) *J. Mol. Biol.* **235,** 545–553
53. Janscak, P., Abadjieva, A., and Firman, K. (1996) *J. Mol. Biol.* **257,** 977–991